Electrochemical DNA Biosensors with Dual Signal Amplification Strategy for Highly Sensitive HPV 16 Detection

Yuxing Yang †, Yazhen Liao †, Yang Qing , Haiyu Li , Jie Du *

Posted Date: 20 July 2023

doi: 10.20944/preprints202307.1357.v1

Keywords: Electrochemical Biosensor; High-risk human papillomavirus; Gold Nanoparticles; 3-Aminopropyltriethoxysilane

Article

Electrochemical DNA Biosensors with Dual Signal Amplification Strategy for Highly Sensitive HPV 16 Detection

Yuxing Yang †, Yazhen Liao †, Yang Qing, Haiyu Li and Jie Du *

College of Materials Science and Engineering, Hainan University, Haikou 570228, China

* Correspondence: author: dujie@hainanu.edu.cn

† These authors contributed equally to this work.

Abstract: Cervical cancer is the most common female reproductive tract tumor and is currently the only cancer that can be prevented by vaccination. Early detection and treatment of cervical cancer can be achieved through regular screening for human papillomavirus (HPV). Therefore, in this paper, an electrochemical sensor was designed to detect HPV 16 using a dual signal amplification technique. APTES modified glassy carbon electrode to improve stability. Combining gold nanoparticles and chain amplification reactions for signal amplification purposes. The limit of detection (LOD) was 1.731×10^{-16} mol/L, and the detection range of this electrochemical sensor was increased in comparison to previous research, with a linear response range from 1.0×10^{-13} mol/L to 1.0×10^{-5} mol/L ($R^2 = 0.99232$) for the target detector.In addition, the sensor showed equally good recovery in sophisticated human serum samples. It shows that it has good interference resistance and the designed biosensor can be a powerful and reliable tool for clinical disease diagnosis.

Keywords: electrochemical biosensor; high-risk human papillomavirus; gold nanoparticles; 3-aminopropyltriethoxysilane

1. Introduction

A significant number of women worldwide pass away each year as a result of cervical cancer, which is a malignant tumor that poses a threat to women's health[1]. Human papillomavirus infection (HPV) causes the vast majority of cervical cancers [2]. HPV is a squamous epithelial hyperplasia spherical DNA virus that causes mucous membrane of human skin. [3]. Depending on the level of pathogenicity, HPV is frequently divided into low-risk and high-risk varieties. High-risk types mainly cause cervical cancer cervical intraepithelial neoplasia, etc. The high-risk subtypes are mainly HPV 16, 18, 31, 56, 59 and 68， and the low-risk types mainly cause skin or genital condyloma, and the main subtypes are HPV 6, 11, 40, 42, 43, 44, 54, 61, 72, 81 and 89.[4]. Research reveal that HPV 16 and HPV 18 are linked to the majority of cervical malignancies[5]. However, it is worth noting that the average age of cervical cancer incidence is gradually decreasing in recent years, with a trend towards younger age[6]. Mortality from cervical cancer continues to rise, especially in developing countries where medical facilities are limited. Consequently, early infection identification can help lower the chance of developing cervical cancer, and cervical cancer diagnosis and testing are both crucial.

Rapid and sensitive detection of specific biomarkers is very important. Gene amplification can raise the concentration of the target to be detected to detectable levels, and routinely used methods include loop-mediated isothermal amplification (LAMP)[7] polymerase chain reaction (PCR)[8] and rolling circle replication (RCA)[9]. These techniques amplify the target DNA sequences to enhance their concentration[10], but they also have drawbacks, such as the need for complex detection equipment, long incubation time, and expensive costs. Because of their great sensitivity, cheap cost, and minimal background signal, electrochemical biosensors have recently been employed to detect HPV as well as other DNA sequences[11–14]. For example, Liu et al. investigated an electrochemical sensor with signal amplification achieved by signal output through hybridization chain reaction

 doi:10.20944/preprints202307.1357.v1

(HCR) to achieve better sensitivity, accuracy and stability[15]. Nucleic acid amplification strategies with electrochemical sensors have been successfully used for nucleic acid detection for nucleic acids [16], small molecules[17] and proteins [18].

3-Aminopropyltriethoxysilane (APTES) is a chemical reagent commonly used to modify substrates by functionalizing their surfaces[19–21]. Modification with APTES can make a good connection between DNA and electrodes and improve the stability of the sensor[22]. Asma Siddique et al. used APTES to link polydimethylsiloxane (PDMS) and proteins to form an APTES coating, which improved cell stability and proliferation using the effect that APTES can stabilize the matrix within the microchannel[23]. Suparat Cotchim and colleagues designed a biosensor modified with APTES to detect trace DNA, and the amine group of APTES interacts with the DNA phosphate backbone to improve the performance of the sensor[24]. In recent years, functionalization with APTES has been a relatively mature technique and has been successfully applied to detect proteins [25], nucleic acids [26]and bacteria[27].

Here, using APTES modified on the surface of a glassy carbon electrode, we created a dual-signal amplified DNA electrochemical biosensor for the detection of HPV 16. In order to prevent the creation of disordered polymers by the hydrolysis of APTES molecules in the system, the performance of the glassy carbon electrode surface was changed with APTES, and the water in the reaction environment was closely regulated. Gold nanoparticles can increase the electrode conductivity[28–30]. The introduction of gold nanoparticles, which take advantage of the high specific surface area of gold nanoparticles, allows more capture probes to be immobilized on the electrode. AP1 and AP2 are two single strands of DNA with base mismatches complementary to each other, which spontaneously undergo strand amplification in the system for signal amplification of the target detectors. According to the experimental results，the sensor has a low detection limit and a boarder detection area, providing a quick and simple method for detecting HPV.

2. Materials and methods

2.1. Instruments

A CS350H electrochemical workstation was used to conduct the electrochemical experiments (Hubei Wuhan Crest Instruments Co., Ltd.). The electrode system used for the experiments was a conventional three-electrode system, with all electrodes procured from Wuhan GOSRELI Technology Co. The electrodes included glassy carbon electrodes with different modifications as working electrodes, platinum wires as auxiliary motors, and Ag/AgCl electrodes as reference electrodes. Scanning electron microscopy (SEM) is used to analyze the surface morphology of electrodes by using the Czech Tescan MIRA LMS, transmission electron microscopy (TEM) was performed by FEI Talos 200S (USA) for sample morphology analysis, and ultraviolet-visible spectrophotometry (UV-Vis) was performed by PE Lambda 750s (USA) for sample analysis.

2.2. Reagents

6-mercapto-1-hexanol (MCH), potassium ferricyanide ($K_3Fe(CN)_6$), potassium chloride (KCl), Magnesium chloride ($MgCl_2$) and sodium chloride (NaCl) were purchased from Aladdin Ltd (Shanghai, China). Sulfuric acid (H_2SO_4), anhydrous ethanol (C_2H_6O) were purchased from Xilong Science Co (Guangzhou, China). Tetrachloroauric acid ($HAuHCl_4$), 3-aminopropyltriethoxysilane (APTES), and tris(2-hydroxyethyl)phosphine (TCEP) were purchased from Shanghai Maclean Biochemical Technology Co (Shanghai, China). Tris-HCl buffer (pH 7.4) was purchased from Biotech Bioengineering (Shanghai) Co. Dichlorotris(1,10-phenanthroline)ruthenium(II) chloride ($[Ru(phen)_3]Cl_2$) was purchased from Sigma Aldrich (Shanghai) Trading Co. Adenosine triphosphate solution (ATP), TE buffer (pH 7.4, 10 mmol/L Tris-HCl, 1 mmol/L EDTA) were purchased from Shanghai Yuan Ye. Trisodium citrate ($C_6H_5O_7Na_3$) is available from Thermo Fisher Scientific. The purity of the purchased chemicals were all of analytical purity. Ultra-pure water (18.25Ω) made from Plus-E3 of Nanjing EPC Technology Development Co., Ltd. was used as the experimental water.

 doi:10.20944/preprints202307.1357.v1

The DNA synthesized by Shanghai Biotechnology Co., Ltd. and purified by HPLC was used in this experiment (Table S1). The DNA was centrifuged first, added TE buffer to solubilize it, and then stored in a 4°C condition.

2.3. Pretreatment of glassy carbon electrode

Prepare the electrode polishing box and moisten the alumina powder poured on the polishing cloth with ultra-pure water to make a paste. Polish the 3mm diameter glassy carbon electrode with 0.3μm and 0.05μm alumina powder in vertical "8" shape until the surface is smooth. Afer five minutes of sonication in ultra-pure water, the electrode was treated in turn with ethanol and ultra-pure water using the same procedure to remove the aluminum oxide particles from the electrode surface.

Cyclic voltammetry (CV) scanning was used to accomplish electrochemical cleaning in 50 mmol/L H2SO4 solution until the curve was steady from -0.4 V to +1.6 V at 0.1 v/s. For use in following tests, the electrode was dried using a powerful hairdryer on cold air setting after being rinsed with ultrapure water.

2.4. Glassy carbon electrodes modified with APTES

The reaction vessel was covered with cling film and incubated for 2 hours with the electrodes submerged in a 1% ethanolic solution of APTES(v/v). The electrode was then taken out, promptly placed in a solution of anhydrous ethanol, and sonicated for 2 minutes.

2.5. Preparation of AuNPs

30mL of 0.01% $HAuHCl_4$ solution was loaded into a washed beaker, stirred continuously with a magnetic stirrer and heated to 120°C in an oil bath. Add 1.5 mL of 1% trisodium citrate solution. 20 minutes later, stop heating and continue stirring until cooled to room temperature to obtain AuNPs solution, which was stored in a 4°C environment for backup.

2.6. Preparation of CP-AuNPs-MCH by freeze-thaw Method

TE buffer is used to make a pH 7.4 DNA fixation buffer that has 500 mmol/L NaCl in it.

Add 6 μL of 10 mmol/L TCEP and 12 μL of 100 μmol/L thiol-modified capture probe (CP), mix well and react for 1 hours. Add 400 μL of 1OD (Optical density) AuNPs solution, mix well and freeze in a refrigerator at -20°C for 2 hours. After freezing, thaw at ambient temperature and centrifuge the thawed solution for 20 minutes at 14,000 rpm. The supernatant was removed with a pipette gun, redissolved in ultrapure water, and repeatedly centrifuged three times to remove excess CP to obtain CP-AuNPs solution.

In order to prevent undesired DNA adsorption, the produced CP-AuNPs solution was centrifuged at 14,000 rpm for 20 minutes. Discard the supernatant of the solution, dissolved it again in 1×10^{-8} mol/L MCH solution, and react for 1 hours. When the reaction was finished, the mixture was centrifuged for 20 minutes at 14,000 rpm, discard the supernatant of the solution and the process was done again to eliminate the MCH reaction that had not yet finished. Centrifugation was performed again, and the supernatant was discarded and dissolved in DNA fixation buffer to 1672 μL. Store the prepared CP-AuNPs-MCH solution in a refrigerator at 4°C.

2.7. Preparation of Sensors

TE buffer was made into DNA hybridization buffer (pH 7.4) by adding 500 mmol/L NaCl and 1 mmol/L $MgCl_2$ to it.

70 μL of CP-AuNPs-MCH solution in a 2 mL centrifuge tube, place the APTES-modified glassy carbon electrode upside down in the tube, incubate overnight on a shaker at 500 rpm (to prevent the electrode from throwing out too fast, using water bath shaking), rinse the electrode and blow dry at the end of the reaction. On the electrode, 10 μL of 10 mmol/L ATP was injected dropwise and reacted for 1 hours. The electrode was blown dry after being cleaned off. The electrode was then washed off and dried after reacting for 2 hours with 10 μL of various target DNA (TD) concentrations that were

Preprints (www.preprints.org) | NOT PEER-REVIEWED | Posted: 20 July 2023 doi:10.20944/preprints202307.1357.v1

applied dropwise. The electrodes were blown dry after washing and incubated in 10 μL of auxiliary DNA 1 (AP1) species for 1 hours. Finally, the combination of 1 μmol/L AP1 and 1 μmol/L auxiliary DNA 2 (AP2), newly made from hybridization buffer. 10 μL drops were taken onto the electrode and allowed to react for 2 hours, then washed off and dried, ready for measurement.

2.8. Electrochemical Measurements

In 0.1 mol/L KCl solution that contains 1 mmol/L $K_3Fe(CN)_6$, cyclic voltammetry experiments were carried out. The voltage was between -0.2 V and 0.6 V, and the scan rate was 50 mV/s. In 10 mmol/L Tris-HCl that contained 5 mmol/L $[Ru(phen)_3]^{2+}$, differential pulse voltammetry measurements were made. The potential was recorded using a range of 0 V to -1 V, a pulse width of 0.05s, a pulse period of 0.1s, an amplitude of 50 mV, and a potential increment of 1mV. I_0 is the peak current in the absence of TD, and I_T is the peak current in the presence of TD, and the signal difference is given as $\Delta I = I_T - I_0$.

3. Results and Discussion

3.1. Structure of the Sensor

Figure 1 shows the flowchart of the idea designed for the program. Firstly, $HAuHCl_4$ solution and trisodium citrate were used for the preparation of gold nanoparticles, and the sulfhydryl-modified CPs were attached to AuNPs by freeze-thaw method. The glassy carbon electrode was subjected to covalent bonding modification using APTES ethanol solution. During the process of self-assembly, APTES molecules were fixed on the electrode surface to create an APTES membrane. The CP-AuNPs might be immobilized on the electrode surface via electrostatic interactions between the phosphate groups on the 5 ends of the DNA single strand and the terminal amino groups of the APTES membrane. Subsequently, one end of TD is hybridized with CP by base complementary pairing and the other end is hybridized with AP1. Since the designed AP1 and AP2 are two single strands of DNA with base mismatch complementarity, they will spontaneously undergo a chain amplification reaction in the system to form a long DNA nanostructure. TD connects this one-dimensional DNA nanostructure to the electrode by hybridization to AP1. Gold nanoparticles have a high specific surface area, which causes more CPs to attach and, in turn, capture more AP1 and AP2 nanostructures. The majority of $[Ru(phen)_3]^{2+}$ also enter the negatively charged DNA double helix structure through electrostatic interactions, which improves the signal value in electrochemical measurements and enables double signal amplification.

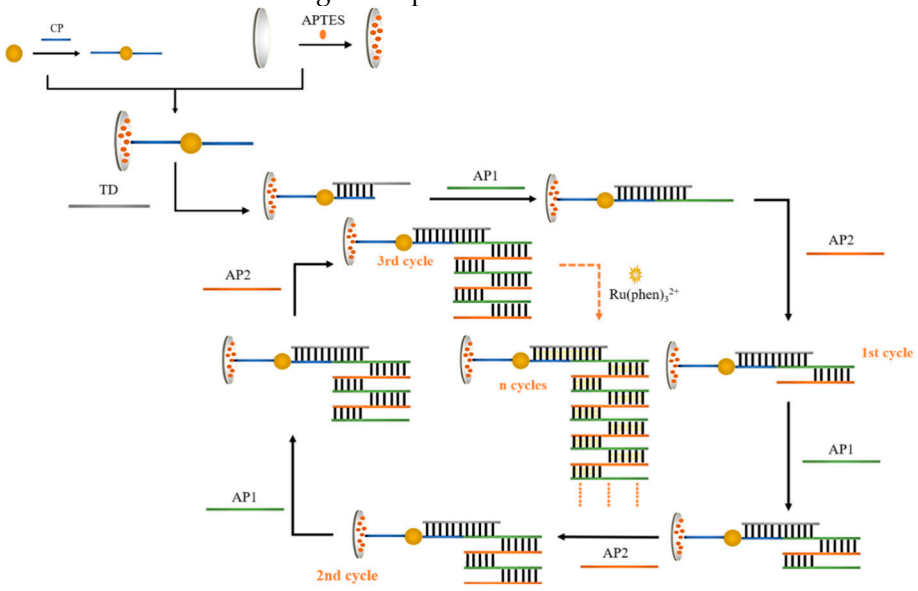

Figure 1. Diagrammatic representation of the dual signal amplified DNA electrochemical biosensor adapted for APTES.

Preprints (www.preprints.org) | NOT PEER-REVIEWED | Posted: 20 July 2023 doi:10.20944/preprints202307.1357.v1

3.2. Electrochemical Characterization

Cyclic voltammetry was used to characterize each step of the experimental operation and was used to determine the completion of each step of the experimental operation. The cyclic voltametric profiles of the glassy carbon electrodes with various degrees of change are shown in Figure 2. The glass carbon electrode modified with the self-assembled APTES film (Figure 2 II) had a higher redox peak than the clean glassy carbon electrode (Figure 2 I), indicating that the electrode modification was successful. Additionally, the system's overall electron transfer efficiency was improved due to APTES' excellent conductivity. When CP-AuNPs (Figure 2 III) are immobilized onto the electrode, although the gold nanoparticles are conductive which increases the electron transfer efficiency, the large number of negatively charged DNA probes attached to the gold nanoparticles makes the electron transfer pathway blocked due to the non-conductive nature of their attached CPs, making the peaks decrease. The DNA double-stranded structure grew as a result of TD hybridization with CPs (Figure 2 IV) and the addition of AP1 and AP2 (Figure 2 V), both of which to various degrees blocked the electron transfer, causing the peaks to progressively decline.

The DPV response signal values of different nucleotide chain modified glassy carbon electrodes are shown in Figure 3. In the context of glassy carbon electrode modified by APTES molecules, the absence of DNA leaves no way for the signal molecule to bind to the electrode and therefore almost no electrochemical signal values are generated. CP-AuNPs are anchored to the electrode surface by the phosphate group at the 5'end of CP binding to the amino group, and since CP is a single chain, $[Ru(phen)_3]^{2+}$ has low binding to CP, thus producing a low value of current response. The hybridization of CP with TD produced double-stranded DNA with only a very small amount of $[Ru(phen)_3]^{2+}$ attached to the double helix structure of DNA and the signal value increases slightly. After the addition of AP1 and AP2 to the system, the electrochemical signal is greatly enhanced by the embedding of large amounts of $[Ru(phen)_3]^{2+}$ after base pairing of TD and AP1 is adsorbed into the double helix structure of the DNA, which immobilizes the long-stranded DNA formed by AP2 and AP1 amplification to the electrode surface. The feasibility of the scheme was demonstrated.

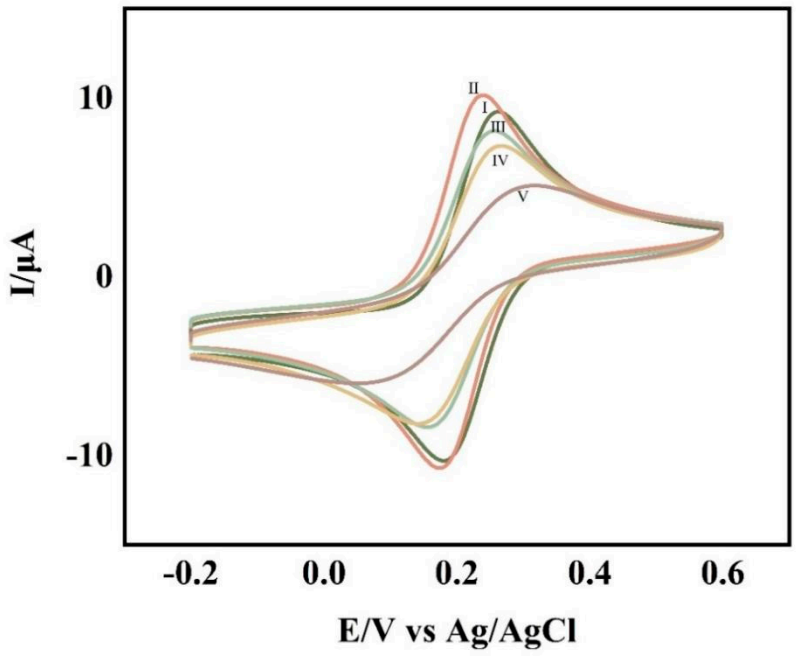

Figure 2. CV at bare GCE(I), GCE/APTES(II), GCE/APTES/CP-AuNPs (III), GCE/APTES/CP-AuNPs/TD(IV), GCE/APTES/CP-AuNPs/TD/AP1/AP2(V) in 0.1mol/L KCl solution containing 1mmol/L $K_3Fe(CN)_6$.

Preprints (www.preprints.org) | NOT PEER-REVIEWED | Posted: 20 July 2023 doi:10.20944/preprints202307.1357.v1

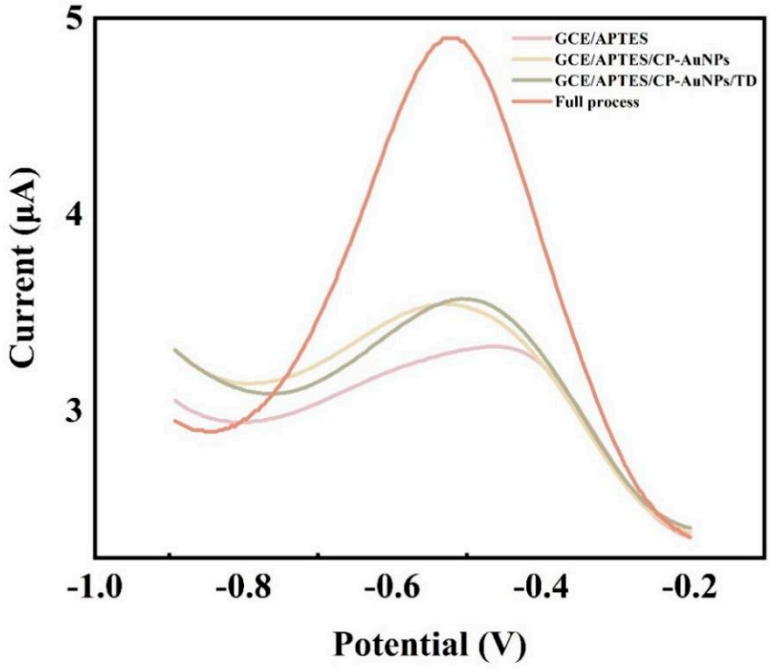

Figure 3. DPV response of oligonucleotide-modified glass carbon electrode in 10 mmol/L Tris-HCl that contained 5 mmol/L $[Ru(phen)_3]^{2+}$. The concentration of TD is 1μmol/L, and AP1 and AP2 are both 1μmol/L as well.

3.3. SEM Characterization of Electrodes.

Analysis of electrode surface morphology by scanning electron microscopy. The surface layer of the APTES-modified glassy carbon electrode displayed a different villi island shape (Figure 4B) when compared to the naked glassy carbon electrode(Figure 4A). By covering the reaction vessel with cling film to stop outside water from entering the reaction system throughout the reaction, the glassy carbon electrode's surface layer, which included hydroxylated silica layer, facilitated the modification of APTES simpler and inhibited the hydrolysis of APTES. The organization order of APTES molecules is susceptible to misalignment because of the weak van der Waals interactions between APTES molecules, which results in APTES films with non-dense internal structure, resulting in a velvety surface.

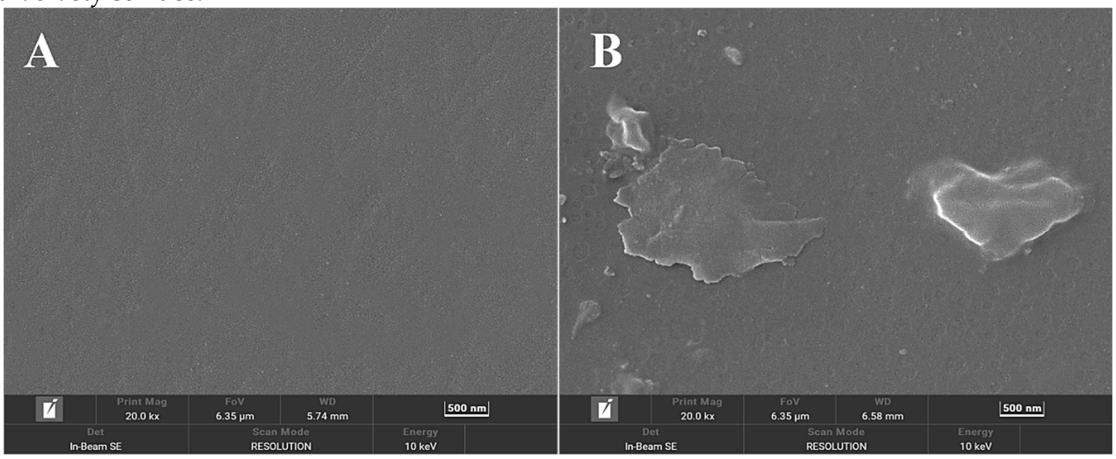

Figure 4. SEM micrographs of (A) bare GCE; (B) GCE/APTES electrodes.

Preprints (www.preprints.org) | NOT PEER-REVIEWED | Posted: 20 July 2023 doi:10.20944/preprints202307.1357.v1

3.4. Characterization of AuNPs

The morphology of the produced AuNPs was studied by transmission electron microscopy. As can be seen in Figure 5, the AuNPs prepared by this experimental method are spherical structures of uniform size, and the average diameter is 16 ± 1 nm using Nano Measurer software for particle size analysis.

The prepared AuNPs were scanned by UV-Vis spectrophotometer in the range of 400–800 nm. as shown in Figure 6, there was an absorption peak at 521 nm. According to the equation of absorption wavelength versus particle size: $\lambda max=0.3647\ D + 515.04$, ($\lambda max$ is the maximum absorption wavelength, D is the particle size) it can be concluded that the particle size of the prepared AuNPs is 16.3 nm.

The conclusions from the transmission electron micrographs and UV-Vis spectroscopy maps are consistent: the AuNPs prepared in this experiment are uniformly distributed spherical particles with a particle size of 16±1 nm.

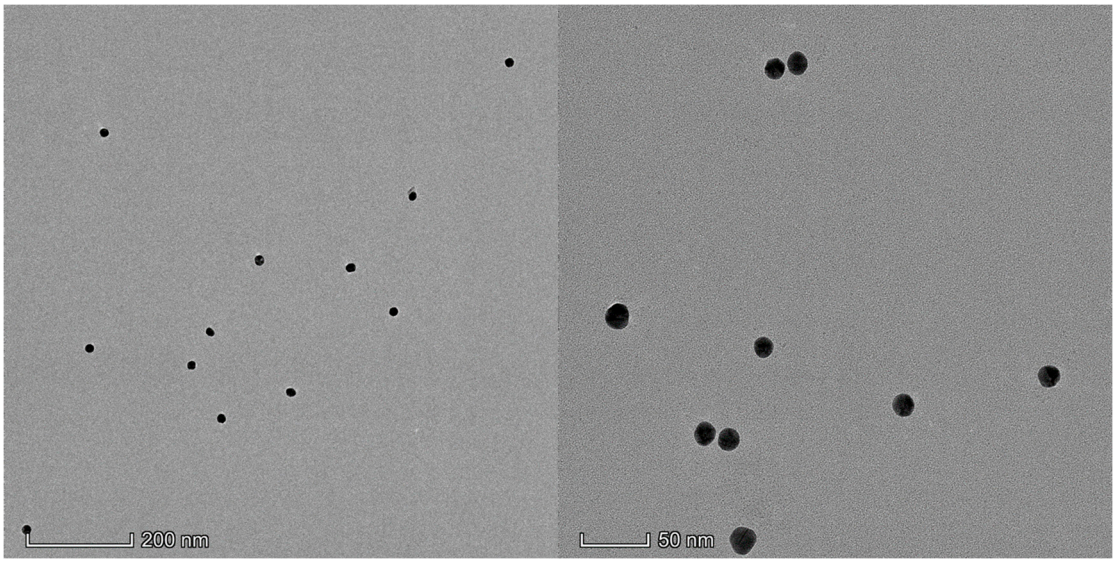

Figure 5. TEM diagram of AuNPs.

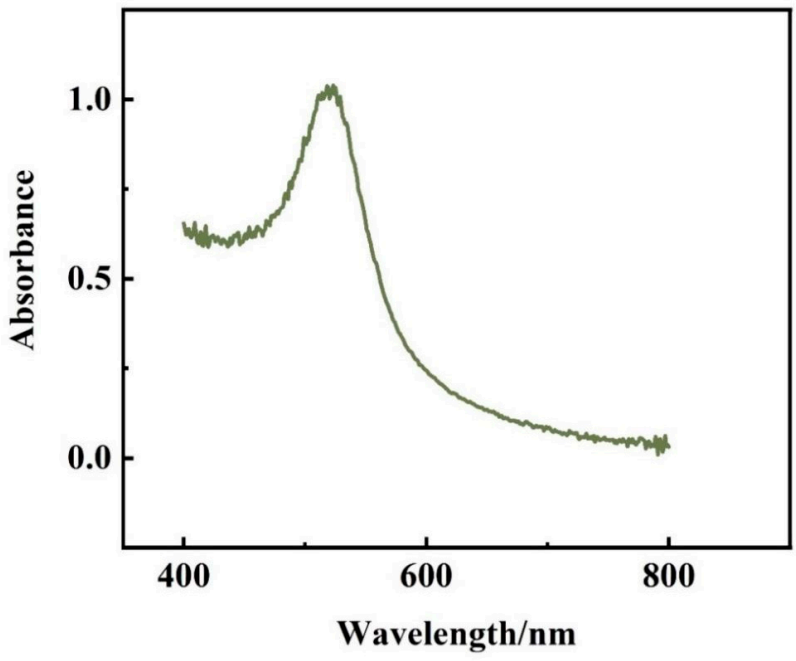

Figure 6. UV-Vis spectroscopy of AuNPs.

Preprints (www.preprints.org) | NOT PEER-REVIEWED | Posted: 20 July 2023 doi:10.20944/preprints202307.1357.v1

3.5. Characterization of Capture Probe Modified AuNPs

After CP was ligated with AuNPs, the prepared CP-AuNPs solution was scanned by UV-Vis spectrophotometer in the range of 400–800 nm. From the Figure 7, the absorption peak at 521 nm was still present, indicating that the linkage of CP with AuNPs did not cause any change in the particle size of AuNPs, i.e., the modification of the probe did not cause aggregation of AuNPs. The difference in absorbance between the two substances is mainly due to the fact that the concentration of the CP-AuNPs solution in which the test was performed is lower than that of the AuNPs solution tested.

In this experiment, AuNPs solution was prepared by trisodium citrate reduction method, as shown in Figure 8. The prepared AuNPs kept the colloid stable showing a clear burgundy color owing to the adsorption of negatively charged citric acid ions on the surface before freeze-thawing. However, the adsorption is not strong, and even the addition of a low concentration of salt (0.25 mol/L NaCl) makes the system irreversibly aggregated, and transparent light blue progressively replaces red in the solution. When the AuNPs solution was frozen, the solution color was clear blue and remained light blue after thawing, indicating that irreversible aggregation of AuNPs occurred. This phenomenon is caused by the fact that when frozen, as the temperature decreases, the water in the solution forms ice crystals, which makes the local concentration of gold nanoparticles increase and form their own agglomerates.

After the CP and AuNPs were mixed thoroughly, the aggregation started to occur with the addition of 0.25 mol/L NaCl solution and the color changed. When adding 0.5 mol/L NaCl solution, the complete aggregation changed to blue color. The fully mixed CP and AuNPs were frozen at -20°C for 2h and thawed at room temperature, and the solution was red, indicating that the solution did not aggregate. Even when 1 mol/L NaCl solution was added, the sample still appeared red, indicating that the mixed solution remained stable without aggregation. It indicates that CP successfully combined with AuNPs and the CP-AuNPs formed a more stable complex after freeze-thawing.

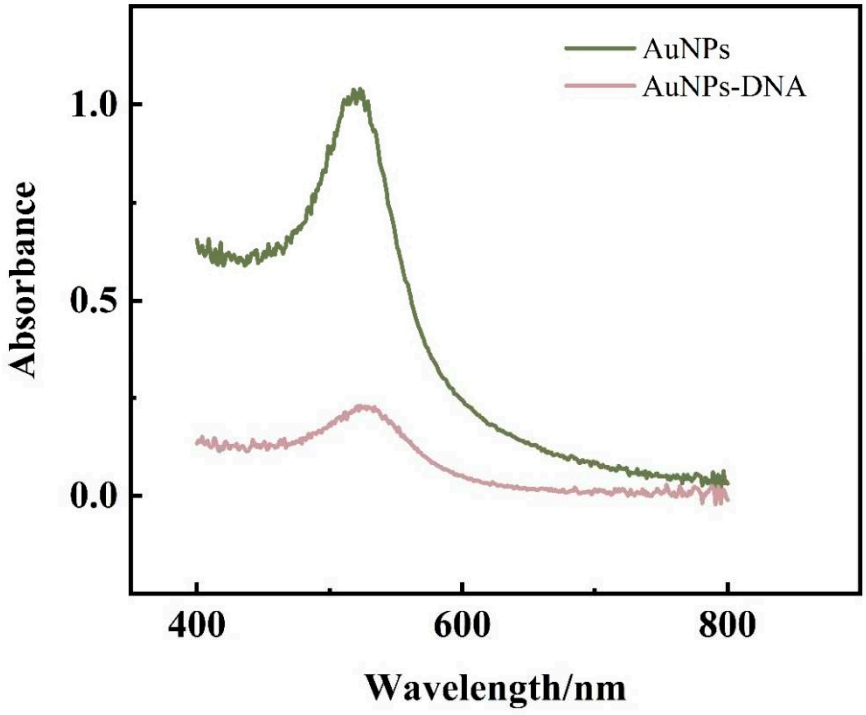

Figure 7. UV-Vis spectroscopy of AuNPs-modified by CP.

Preprints (www.preprints.org) | NOT PEER-REVIEWED | Posted: 20 July 2023 doi:10.20944/preprints202307.1357.v1

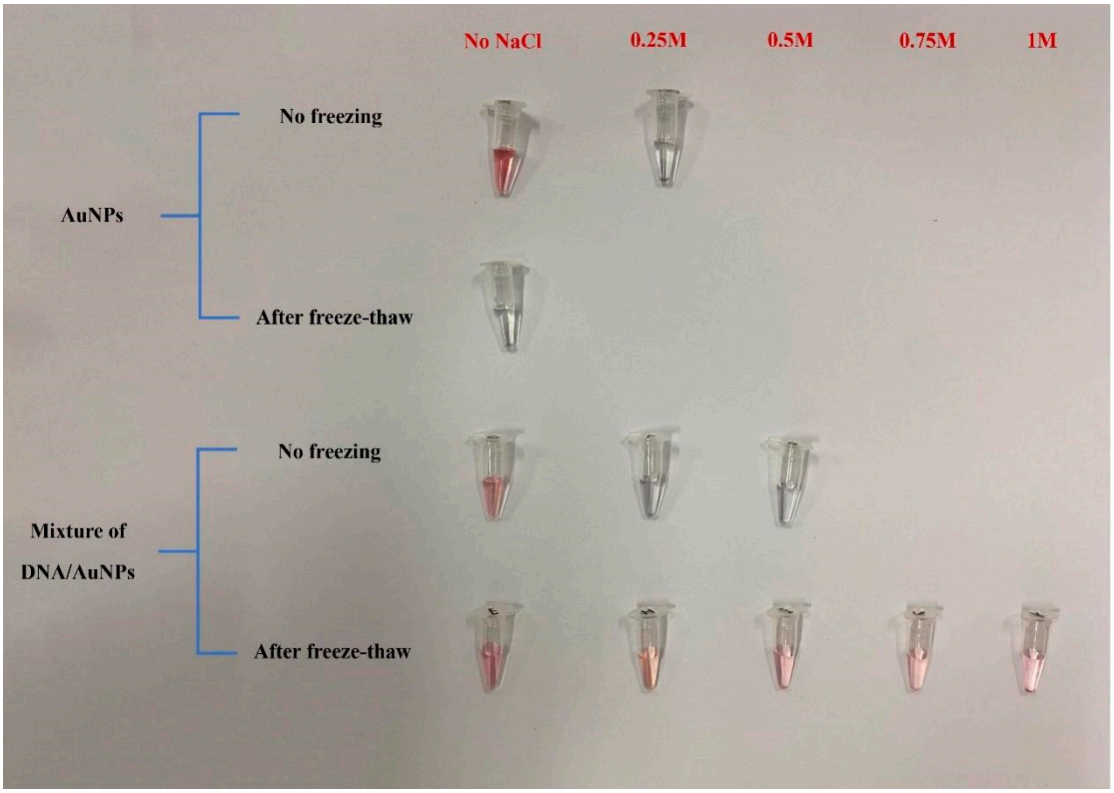

Figure 8. Aggregation of different AuNPs before and after freeze-thaw method.

3.6. Improving Experimental Conditions

The performance of this biosensor was optimized by using a single variable technique, which also ensured the best detection outcomes. To facilitate error analysis, three replicate experiments were conducted for each experiment.

First, the concentration and time of APTES-modified glassy carbon electrode were optimized. The analysis results showed that (Figure 9A), under the strict control of water in the external environment, because the small substrate surface area of the glassy carbon electrode, the APTES molecular weight required to form the self-assembled membrane was small, and 1% concentration of APTES solution could meet the experimental requirements, and the signal value was not significantly enhanced as the concentration increased, so 1% APTES ethanol solution was determined as the best modification concentration for this experiment. After the concentration was determined, the reaction time of APTES was optimized. Theoretically, after the membrane was formed by self-assembly, extending the reaction time did not change the structure and properties of the membrane. However, the reaction time should not be too long because APTES molecules tend to hydrolyze to produce disordered polymers deposited on the substrate surface. From the experimental results (Figure 9B), the signal value remained basically stable after 2 hours of system reaction, thus determining 2 hours as the modification time of APTES. The signal value stopped changing after 2 hours of reaction in this experiment, which employed a 1 μmol/L AP1 and AP2 mixed solution for time optimization. This indicates that AP1 and AP2 completely interacted, and 2 hours was found to be the best reaction time（Figure 9C）. Since the TD concentrations detected in the experiments were different, a larger concentration of 10 μmol/L (none of the TD concentrations in the subsequent experiments would be larger than 10 μmol/L) was selected for time optimization, and it can be seen from Figure 9D that the 10 μmol/L TD solution reacted completely at 2 hours. Therefore, 2 hours was determined as the incubation time of the target substance.

Preprints (www.preprints.org) | NOT PEER-REVIEWED | Posted: 20 July 2023 doi:10.20944/preprints202307.1357.v1

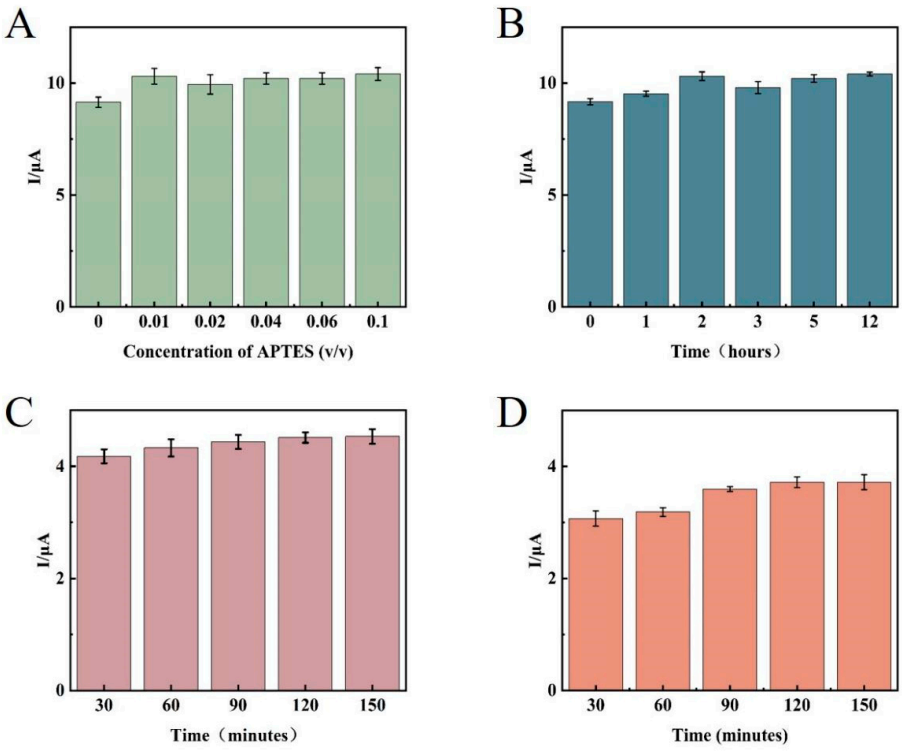

Figure 9. Effects of (A) concentration of the APTES; (B) APTES reaction time; (C) incubation time of AP1 and AP2; (D) incubation time of TD.

3.7. Sensor Performance

With the optimal experimental conditions obtained above, a gradient of DPV concentration was performed for the target detector (HPV 16). Given as the ideal reaction time, the current response value of the DPV steadily rose with the rise in TD concentration from 1.0×10^{-14} mol/L to 1.0×10^{-5} mol/L, as shown in Figure 10A. As the amplification grows and expands, more signal molecules $[Ru(phen)_3]^{2+}$ are inserted into the double helix structure of the DNA, acting as an amplifier of the signal. This suggests that more target DNA is immobilized on the electrode, allowing more long-stranded DNA to be attached to the electrode. A satisfactory linear association between the DPV signal value and the target DNA concentration from 1.0×10^{-13} mol/L to 1.0×10^{-5} mol/L was found by fitting the linear regression data (Figure 10B), with the regression equation $\Delta I = 0.08611 \log C_{TD} + 4.33051$ ($R^2 = 0.9923$). The detection limit of this electrochemical biosensor may be estimated using the regression equation $LOD=3\sigma/S=1.731\times10^{-16}$mol/L (where the standard deviation of the blank sample set is denoted as σ and the slope of the fitted line in the inset of Figure 10B is denoted as S). Comparing the current study to other previously reported biosensors for the detection of HPV 16 as well as to the prior procedure, it revealed a lower detection limit and a wider linear range (as shown in Table 1). The aforementioned findings imply that this DNA electrochemical biosensor can detect target DNA with excellent sensitivity and a broad linear range.

Table 1. The proposed sensor is compared with other sensors for the detection of HPV 16.

Dynamic Line arrange(mol/L)	LOD(mol/L)	Method	Reference
3.50×10^{-12} -3.53×10^{-11}	1.750×10^{-12}	DPV	[31]
5.00×10^{-10} -1.00×10^{-7}	1.500×10^{-10}	DPV	[32]
1.00×10^{-14} -1.00×10^{-6}	1.000×10^{-15}	EIS	[33]
1.00×10^{-10} -2.00×10^{-7}	3.000×10^{-11}	ECL	[34]
1.00×10^{-13} -1.00×10^{-6}	5.475×10^{-16}	DPV	[35]
1.00×10^{-13} -1.00×10^{-5}	1.731×10^{-16}	DPV	This work

Preprints (www.preprints.org) | NOT PEER-REVIEWED | Posted: 20 July 2023 doi:10.20944/preprints202307.1357.v1

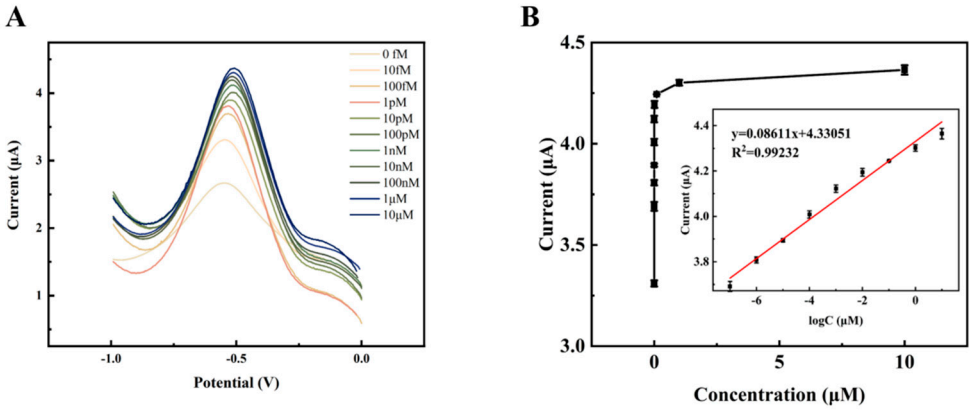

Figure 10. (A)Several TD concentrations (1.0×10^{-14}, 1.0×10^{-13}, 1.0×10^{-12}, 1.0×10^{-11}, 1.0×10^{-10}, 1.0×10^{-9}, 1.0×10^{-8}, 1.0×10^{-7},1.0×10^{-6},1.0×10^{-5} mol/L) were detected in the DPV signals. (B) Association between DPV intensities and TD concentrations. Insert: calibration curve between the logarithm of TD concentrations and ΔI.

3.8. Sensor Selectivity and Stability

In this study, the selective expression of this DNA electrochemical biosensor was investigated by comparing sample solutions of eight different DNA sequences, each consisting of three parallel sets of experiments for error analysis. Figure 11 displays how well this sensor selects various targets. Compared to the concentration of other DNA sequences, the concentration of TD chosen for the experiment is ten times lower. The peak current intensity of the DPV assay in the blank control was only slightly lower than that of the assays containing 2MT, 1MT, NC, HPV 33, HPV 31 and HPV 18, but much lower than that of the TD assay. The low signal value indicates that the sensing system is highly selective for the target HPV 16 and prevents the influence of non-target DNA sequences on the detection results. This indicates that the probe created by the sensor cannot hybridize and pair with other DNA base sequences, and the amplification product cannot connect with the electrode in the absence of the target DNA.

The stability of the electrochemical DNA biosensor was also examined under ideal circumstances. The electrochemical tests were conducted on day 1 when the sensor preparation was completed and on days 7 and 14 when it was left at 4°C. From Figure 12, the current response value decreased by only 1.008% after 7 days and by only 2.420% after 14 days, indicating the good stability of the electrochemical biosensor.

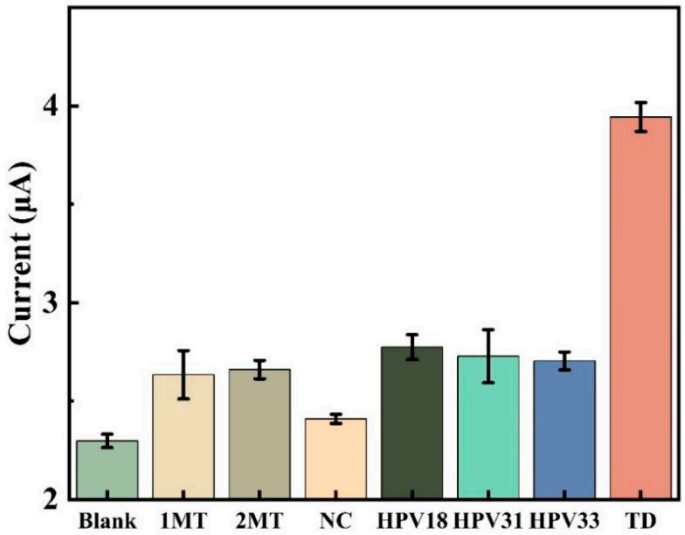

Figure 11. Comparison of DPV reactions for various DNA (NC,2MT, 1MT, HPV33, HPV31, HPV18, TD) and blank sample sets. TD concentration is 1nmol/L, other sample concentrations are 10nmol/L.

Preprints (www.preprints.org) | NOT PEER-REVIEWED | Posted: 20 July 2023 doi:10.20944/preprints202307.1357.v1

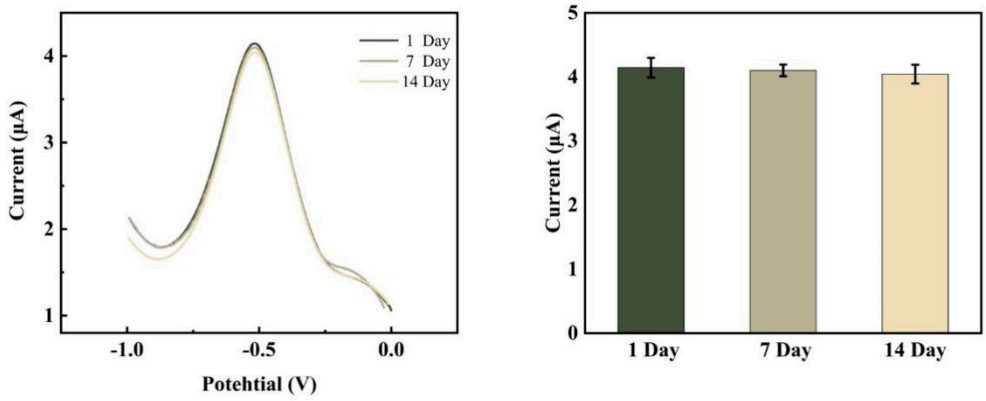

Figure 12. DPV reaction prior to and following the sensor's placement at 4°C for 7 days and 14 days, respectively.

3.9. Detection in Real Samples

The capacity of a sensor to detect in challenging settings, such blood serum, is one of the key metrics. To test the detection capabilities of the sensor, various concentrations of TD (1, 10, 100 nmol/L) were added to the serum solution for recovery tests. Table 2 presents the outcomes. From 98.70% to 100.53% is the range of recovery and 1.74% to 3.14% is the relative standard deviation (RSD) of recovery. This indicates that the sensor still has outstanding detection capability as well as good interference immunity in complex environments.

Table 2. The serum sample were tested for HPV 16.

TD added(nmol/L)	Total found (nmol/L)	Recovery (%)	RSD (%)
1.0	0.987	98.70	1.74
10.0	9.985	99.85	3.14
100.0	100.533	100.53	1.95

4. Conclusions

In this experiment, the substrate used is glassy carbon electrode, and APTES was used to construct the self-assembled membrane on the glassy carbon substrate by covalent bonding to obtain a more stable biosensor system for HPV 16 detection. After placing the sensor for 7 days, the current corresponding value only decreased by 1.008%, and after 14 days, the current response value only decreased by 2.420%, which is more stable. The sensor's sensitivity is increased by dual signal amplification by gold nanoparticles and chain amplification reaction. The sensor sensing range is from 1.0×10^{-13} mol/L to 1.0×10^{-5} mol/L, and the detection limit of the sensor is 1.731×10^{-16} mol/L. The ligation of DNA and gold nanoparticles by freeze-thaw method is simpler and faster compared to the conventional salt aging method. Moreover, the sensor has great detection capabilities in both selective and complex contexts, which has practical application in clinical testing and generates fresh insights for illness detection and diagnosis.

Author Contributions: Y.Y., Y.L., H.L. and J.D. performed the experiments and wrote the paper; Y.Y., Y.L., Y.Q. and H.L. analyzed the data, and J.D. conceived and designed the experiments.

Funding: This work was financially supported by Hainan Province Science and Technology Special Fund (ZDYF2023SHFZ110), the National Natural Science Foundation of China (Grant No. 21763009, 21404028), and Graduate Students Innovation Research Project of Hainan Province (Hys2020-35).

Acknowledgments: Sincere gratitude to Hui Zhang, Zhencui Wang, Bingbing Wang, Haobin Fang, Xiaoxue Yin and Xinxin Liu for their assistance in this work.

Conflicts of Interest: The authors declare no conflicts of interest.

References

1. Allanson: E. R.; Schmeler, K. M., Preventing Cervical Cancer Globally: Are We Making Progress? Cancer Prev Res (Phila) 2021, 14, (12), 1055-1060.
2. Kovachev, S.; Slavov, V., Prevalence of human papillomavirus infection in women in Bulgaria: A 2017 update. J Med Virol 2018, 90, (6), 1142-1149.
3. Graham, S. V., Human Papillomavirus E2 Protein: Linking Replication, Transcription, and RNA Processing. J Virol 2016, 90, (19), 8384-8.
4. Han, K. H., Evaluation of human papillomavirus (HPV) genotyping assays using type-specific HPV L1 reference DNA. Genes Genomics 2021, 43, (7), 775-781.
5. Brotherton, J. M. L.; Tabrizi, S. N.; Phillips, S.; Pyman, J.; Cornall, A. M.; Lambie, N.; Anderson, L.; Cummings, M.; Payton, D.; Scurry, J. P.; Newman, M.; Sharma, R.; Saville, M.; Garland, S. M., Looking beyond human papillomavirus (HPV) genotype 16 and 18: Defining HPV genotype distribution in cervical cancers in Australia prior to vaccination. Int J Cancer 2017, 141, (8), 1576-1584.
6. Xi, C.; Shen, J. J.; Burston, B.; Upadhyay, S.; Zhou, S., Epidemiological/Disease and Economic Burdens of Cervical Cancer in 2010-2014: Are Younger Women at Risk? Healthcare (Basel) 2023, 11, (1).
7. Khan, M. J. R.; Bhuiyan, M. A.; Tabassum, S.; Munshi, S. U., Use of whole blood and dried blood spot for detection of HIV-1 nucleic acids using reverse transcription loop-mediated isothermal amplification. Journal of Virological Methods 2023, 312.
8. Wei, J.; Zhou, X.; Xing, D.; Wu, B., Rapid and sensitive detection of Vibrio parahaemolyticus in sea foods by electrochemiluminescence polymerase chain reaction method. Food Chemistry 2010, 123, (3), 852-858.
9. Xu, H.; Wu, D.; Zhang, Y.; Shi, H.; Ouyang, C.; Li, F.; Jia, L.; Yu, S.; Wu, Z.-S., RCA-enhanced multifunctional molecule beacon-based strand-displacement amplification for sensitive microRNA detection. Sensors and Actuators B: Chemical 2018, 258, 470-477.
10. Xia, Y.; Huang, Z.; Chen, T.; Xu, L.; Zhu, G.; Chen, W.; Chen, G.; Wu, S.; Lan, J.; Lin, X.; Chen, J., Sensitive fluorescent detection of exosomal microRNA based on enzymes-assisted dual-signal amplification. Biosens Bioelectron 2022, 209, 114259.
11. Hai, X.; Li, Y.; Zhu, C.; Song, W.; Cao, J.; Bi, S., DNA-based label-free electrochemical biosensors: From principles to applications. TrAC Trends in Analytical Chemistry 2020, 133.
12. Sun, Y.; Liu, J.; Peng, X.; Zhang, G.; Li, Y., A novel photoelectrochemical array platform for ultrasensitive multiplex detection and subtype identification of HPV genes. Biosens Bioelectron 2023, 224, 115059.
13. Liao, Y.; Gao, J.; Huang, W.; Yuan, R.; Xu, W., LAMP-H(+)-responsive electrochemical ratiometric biosensor with minimized background signal for highly sensitive assay of specific short-stranded DNA. Biosens Bioelectron 2022, 195, 113662.
14. Chai, H.; Tang, Y.; Guo, Z.; Miao, P., Ratiometric Electrochemical Switch for Circulating Tumor DNA through Recycling Activation of Blocked DNAzymes. Anal Chem 2022, 94, (6), 2779-2784.
15. Chen Liu , T. W., Wei Zeng , Jingmin Liu , Bing Hu , Long Wua,, Dual-signal electrochemical aptasensor involving hybridization chain reaction amplification for aflatoxin B1 detection. Sensors and Actuators: B. Chemical 2022, 371.
16. Shengqiang Li ; Zhengxiang Fu ; Chao Wang ; Xipeng Shang ; Yan Zhao; Cuiying Liu c; ., M. p., An ultrasensitive and specific electrochemical biosensor for DNA detection based on T7 exonuclease-assisted regulatory strand displacement amplification. Analytica Chimica Acta 2021, 1183.
17. Pei, Q.; Song, X.; Liu, S.; Wang, J.; Leng, X.; Cui, X.; Yu, J.; Wang, Y.; Huang, J., A facile signal-on electrochemical DNA sensing platform for ultrasensitive detection of pathogenic bacteria based on Exo III-assisted autonomous multiple-cycle amplification. The Analyst 2019, 144, (9), 3023-3029.
18. Qing, M.; Sun, Z.; Wang, L.; Du, S. Z.; Zhou, J.; Tang, Q.; Luo, H. Q.; Li, N. B., CRISPR/Cas12a-regulated homogeneous electrochemical aptasensor for amplified detection of protein. Sensors and Actuators B: Chemical 2021, 348.
19. Bourkaib, M. C.; Gaudin, P.; Vibert, F.; Guiavarc'h, Y.; Delaunay, S.; Framboisier, X.; Humeau, C.; Chevalot, I.; Blin, J.-L., APTES modified SBA15 and meso-macro silica materials for the immobilization of aminoacylases from Streptomyces ambofaciens. Microporous and Mesoporous Materials 2021, 323.
20. Nayak, N.; Huertas, R.; Crespo, J. G.; Portugal, C. A. M., Surface modification of alumina monolithic columns with 3-aminopropyltetraethoxysilane (APTES) for protein attachment. Separation and Purification Technology 2019, 229.
21. Victor V.C. Lima, F. B. D. N., Enrique C. Peres, Glaydson S. Reis, Éder C. Lima, Marcos L.S. Oliveirac, Guilherme L. Dotto,, Synthesis and characterization of biopolymers functionalized with APTES (3–aminopropyltriethoxysilane) for the adsorption of sunset yellow dye. Journal of Environmental Chemical Engineering 2019, 7.
22. Ghazali, N. N.; Mohamad Nor, N.; Abdul Razak, K.; Lockman, Z.; Hattori, T., Hydrothermal synthesis of bismuth nanosheets for modified APTES-functionalized screen-printed carbon electrode in lead and cadmium detection. Journal of Nanoparticle Research 2020, 22, (7).

23. Siddique, A.; Meckel, T.; Stark, R. W.; Narayan, S., Improved cell adhesion under shear stress in PDMS microfluidic devices. Colloids Surf B Biointerfaces 2017, 150, 456-464.
24. Cotchim, S.; Thavarungkul, P.; Kanatharana, P.; Thanakiatkrai, P.; Kitpipit, T.; Limbut, W., Extraction and electrochemical detection for quantification of trace-level DNA. Mikrochim Acta 2021, 188, (6), 180.
25. Nur Sonuç Karaboğa, M.; Kemal Sezgintürk, M., A Practical Approach for the Detection of Protein Tau with a Portable Potentiostat. Electroanalysis 2022.
26. Ebrahim, S.; Raoof, M.; Ramadan, W.; Soliman, M., New self assembly monolayer onto SiGe as a selective biosensor for single-strand DNA. Microelectronic Engineering 2016, 160, 87-93.
27. Deshmukh, R.; Prusty, A. K.; Roy, U.; Bhand, S., A capacitive DNA sensor for sensitive detection of Escherichia coli O157:H7 in potable water based on the z3276 genetic marker: fabrication and analytical performance. Analyst 2020, 145, (6), 2267-2278.
28. Khater, M.; de la Escosura-Muniz, A.; Quesada-Gonzalez, D.; Merkoci, A., Electrochemical detection of plant virus using gold nanoparticle-modified electrodes. Anal Chim Acta 2019, 1046, 123-131.
29. Pilehvar, S.; Reinemann, C.; Bottari, F.; Vanderleyden, E.; Van Vlierberghe, S.; Blust, R.; Strehlitz, B.; De Wael, K., A joint action of aptamers and gold nanoparticles chemically trapped on a glassy carbon support for the electrochemical sensing of ofloxacin. Sensors and Actuators B: Chemical 2017, 240, 1024-1035.
30. Pourmadadi, M.; Shayeh, J. S.; Omidi, M.; Yazdian, F.; Alebouyeh, M.; Tayebi, L., A glassy carbon electrode modified with reduced graphene oxide and gold nanoparticles for electrochemical aptasensing of lipopolysaccharides from Escherichia coli bacteria. Mikrochim Acta 2019, 186, (12), 787.
31. Chekin, F.; Bagga, K.; Subramanian, P.; Jijie, R.; Singh, S. K.; Kurungot, S.; Boukherroub, R.; Szunerits, S., Nucleic aptamer modified porous reduced graphene oxide/MoS2 based electrodes for viral detection: Application to human papillomavirus (HPV). Sensors and Actuators B: Chemical 2018, 262, 991-1000.
32. Jampasa, S.; Siangproh, W.; Laocharoensuk, R.; Yanatatsaneejit, P.; Vilaivan, T.; Chailapakul, O., A new DNA sensor design for the simultaneous detection of HPV type 16 and 18 DNA. Sensors and Actuators B: Chemical 2018, 265, 514-521.
33. Shariati, M.; Ghorbani, M.; Sasanpour, P.; Karimizefreh, A., An ultrasensitive label free human papilloma virus DNA biosensor using gold nanotubes based on nanoporous polycarbonate in electrical alignment. Analytica Chimica Acta 2019, 1048, 31-41.
34. Nie, Y.; Zhang, X.; Zhang, Q.; Liang, Z.; Ma, Q.; Su, X., A novel high efficient electrochemiluminescence sensor based on reductive Cu(I) particles catalyzed Zn-doped MoS2 QDs for HPV 16 DNA determination. Biosens Bioelectron 2020, 160, 112217.
35. Yang, Y.; Qing, Y.; Hao, X.; Fang, C.; Ouyang, P.; Li, H.; Wang, Z.; Liao, Y.; Fang, H.; Du, J., APTES-Modified Remote Self-Assembled DNA-Based Electrochemical Biosensor for Human Papillomavirus DNA Detection. Biosensors 2022, 12, (7).